Using N-nitrosodiethanolamine (NDELA) and N-nitrosopiperidine (NPIP) transgenic rodent gene mutation data and quantum mechanical modeling to derive potency-based acceptable intakes for NDSRIs lacking robust carcinogenicity data

Jason M. Roper[1], Troy R. Griffin[1], George E. Johnson[2], Jakub Kostal[3], Raphael Nudelman[4], Gregory R. Ott[1], Adelina Voutchkova-Kostal[3],Valerie Niddam-Hildesheim[5]

Short Running Title: Acceptable intakes for NDSRIs based on in vivo mutagenic potency and quantum mechanical modeling

Keywords: Benchmark Dose, Nitrosamine, Risk Assessment, Critical Effect Size, TGR

Author Affiliations:

[1]Teva Branded Pharmaceuticals R&D, Inc., West Chester, Pennsylvania, USA

[2]Swansea, Wales, United Kingdom

[3]Designing Out Toxicity (DOT) Consulting LLC, Alexandria, Virgina, USA

[4]Nudelman ChemTox Consulting, Rehovot, Israel

[5]Teva Pharmaceutical Industries Ltd., Tel Aviv 6944020, Israel

Corresponding Author: Jason M. Roper, PhD, Nonclinical Development, Teva Branded Pharmaceuticals R&D, Inc., West Chester, PA. Email: jason.roper@tevapharm.com

ABSTRACT

Acceptable intake (AI) limits for nitrosamine drug substance related impurities (NDSRIs) that lack carcinogenicity data could be estimated from mutagenic potency relative to anchor nitrosamines with carcinogenicity data. This approach integrates points of departure (PoDs) derived from *in vivo* mutagenicity studies with *in silico* predictions generated by a validated quantum-mechanical (QM) model. N-nitrosodiethanolamine (NDELA) and N-nitrosopiperidine (NPIP), with acceptable intakes (AIs) derived from robust carcinogenicity data, were tested in the transgenic rodent (TGR) gene mutation assay. Liver mutant frequency and benchmark dose (BMD) modeling provided a suitable, robust, and precise PoD metric. BMD confidence intervals (CIs) calculated from mutant frequency expanded the potency range of previously reported BMD CIs for other anchor nitrosamines. Cancer-protective AIs for mutagenic NDSRIs can be pragmatically calculated on a potency basis by comparing their lower bound TGR BMD CIs with the BMD CIs and AIs derived from model/anchor nitrosamines that have results for *in vivo* gene mutation and cancer bioassays. *In vivo* modeling was supported by the Computer-Aided Discovery and RE-design (CADRE) program, a validated QM model for predicting NDSRI carcinogenic potency based on the underlying mechanism of mutagenicity. CADRE distinguished between anchor nitrosamines N-nitrosodiethylamine (NDEA) and N-nitrosodimethylamine (NDMA) and the less potent NDELA and NPIP. Scrutiny of underlying reactivity indices and relevant physicochemical properties rationalized the observed trend in metabolic activity and thus predicted carcinogenic potency. Leveraging the *in vivo-in silico* approach is valuable in gaining confidence in the proposed AIs, whereby the QM model serves as mechanistic validation of *in vivo* results.

1. INTRODUCTION

Nitrosamines, including some nitrosamine drug substance-related impurities (NDSRIs), often possess mutagenic potential. Carcinogenic nitrosamines have a wide range of doses associated with a 50% tumor incidence (TD_{50}), and therefore, as a class, possess varying carcinogenic potencies (Thresher et al., 2020). A number of these substances have been assessed using the *in vivo* transgenic rodent (TGR) gene mutation assay (OECD, 2022), and benchmark dose (BMD) confidence intervals (CI) have subsequently been calculated from their dose responses (Bercu et al., 2023a; Jolly et al., 2024; Lynch et al., 2024; Powley et al., 2024). It is therefore possible to consider that these animal-based metrics could be extrapolated to human risk by application of adjustments and uncertainty factors commonly used to derive health-based guidance values (Jolly et al., 2024; Powley et al., 2024).

The current default approach for assessment and control of DNA reactive impurities in pharmaceuticals (ICH, 2023) is to use a predefined acceptable intake (AI) with adjustments for clinical use scenarios and treatment duration. In cases where robust cancer bioassay data are available (e.g. Class 1 impurities), a substance-specific AI should be calculated using carcinogenic potency by linear extrapolation from a defined TD_{50}, a threshold value representing the dose expected to produce a 50% tumor incidence in the study population, to an acceptable lifetime cancer risk (1 in 100,000) for humans (EMA, 2024). As an alternative method, and in order to better account for the shape of the dose-response curve of the carcinogenicity data, the ICH M7 guidance for assessment and control of DNA reactive (mutagenic) impurities allows for the use of a BMD in lieu of TD_{50} values as a numerical index for carcinogenic potency (ICH, 2023). However, as clarified in ICH M7 Questions and Answers (ICH, 2022), *in vivo* gene mutation assays alone are currently not considered valid to support direct assessment of carcinogenic risk because the primary endpoint is mutation and not carcinogenicity.

The concept of relative potency, wherein dose ranges associated with scientifically meaningful fractional increases in mutagenic response from *in vivo* mutation data (BMD) are compared against TD_{50} values calculated from cancer bioassay data, has recently been assessed for multiple nitrosamines (Johnson et al., 2021; Thomas et al., 2025). From a regulatory perspective, Chepelev et al. (2023) demonstrated that risk management decisions based on *in vivo* genotoxicity dose-response data would be comparable to, or slightly more conservative than decisions based on carcinogenicity dose-response data. It is therefore reasonable to consider that this relative potency concept would be similarly applicable to data generated for mutagenic nitrosamines, including NDSRIs, and that using AIs derived from *in vivo* mutation threshold values would be comparably health protective compared with current methods.

As focus has shifted from small, process-related nitrosamine risks to NDSRIs, where robust cancer bioassay data are not available and are unlikely to be generated, derivation of a defensible AI has become challenging within the current regulatory framework. The resultant application of AI values derived using *in silico* approaches such as structure-based read-across to more potent nitrosamines with cancer bioassay data (EMA, 2024), or sub-structural predictive models like the Carcinogenic Potency Category Approach (CPCA) (Kruhlak et al., 2024), are conservative by design and may be over-predictive for higher molecular weight, structurally-complex NDSRIs (Chakravarti et al., 2024; Ponting et al., 2024). We hypothesize that by directly linking nitrosamine carcinogenicity to its mutagenic potential, more accurate and precise AI values can be calculated using substance-specific *in vivo* mutagenicity data with a BMD modeling approach if a dose range associated with a scientifically meaningful fractional increase for the mutagenic response can be identified.

A pragmatic, scientifically-based approach to the calculation of health-protective AIs for mutagenic NDSRIs lacking carcinogenicity bioassay data would be to leverage the empirical relationship between carcinogenic potency (as assessed by the AIs derived from carcinogenicity TD_{50} values) and mutagenic potency (as assessed by *in vivo* mutagenicity assays) using AIs derived from TD_{50} values associated with robust carcinogenicity bioassays and BMD values from well conducted *in vivo* mutagenicity assays for model/anchor nitrosamines. Recently, BMD CIs derived from *in vivo* TGR mutagenicity data have been published for N-nitrosodimethylamine (NDMA; Lynch et al., 2023), and N-nitrosodiethylamine (NDEA; Bercu et al., 2023a), two small similarly-potent genotoxic and carcinogenic nitrosamines with AI values ranging from 96 to 145 ng/day for NDMA and 26.5 to 62 ng/day for NDEA, respectively (Bercu et al., 2023b; EMA, 2024). Consistent with ICH M7 Questions and Answers (ICH, 2022), the resultant AIs can be supported by a validated quantum-mechanical (QM) model that is predictive of carcinogenic potency by capturing the mechanism of *in vivo* mutagenicity using electronic structure theory. In that regard, the use of QM was embraced by the regulator to both validate and potentially expand the CPCA, further justifying it applicability in AI calculations (CRCG, 2024; FDA, 2024). An appropriate model should satisfy the OECD guidelines for (Quantitative) Structure-Activity Relationships (Q)SARs, (OECD, 2014) and conceptually align with the regulator-accepted SARs in the CPCA. The Computer-Aided Discovery and Redesign (CADRE) tool was developed for this purpose, and was externally validated in a previous study (Kostal and Voutchkova-Kostal, 2023). In contrast to the CPCA, which is a rule-based SAR, CADRE uses QM and mixed QM/MM (Quantum and Molecular Mechanics) calculations to relate key events in the nitrosamine metabolism to banker bioassay data (TD_{50}) in a statistical approach. With reactivity metrics assessed *ab initio* (i.e. from first principles), CADRE is accurate

outside current knowledge (ca. 77% in assigning carcinogenic potency), which is critical when extrapolating from small nitrosamines to the larger and more complex NDSRIs (Kostal et al., 2024; Kostal and Voutchkova-Kostal, 2023).

The objective of the work presented herein was to complement the prior NDMA and NDEA studies by conducting CADRE/QM analysis and *in vivo* TGR assays with two additional small molecular weight anchor nitrosamines, N-nitrosodiethanolamine (NDELA, MW: 134.14 g/mol) and N-nitrosopiperidine (NPIP, MW: 114.1 g/mol), which have carcinogenicity potencies approximately 10-fold weaker than NDMA and NDEA. The choice of test substances was based on the relative paucity of nitrosamines for which there are robust carcinogenicity data, and to expand the range of substances with comparative *in vivo* mutagenicity and carcinogenicity data to include those with lower apparent carcinogenic potencies. Concurrent with these investigations, NPIP was also recently evaluated in a different transgenic *in vivo* test system (BigBlue® rat; Powley et al., 2024). Regulatory AIs for NDELA and NPIP (1900 and 1300 ng/day, respectively) were calculated from the most sensitive TD_{50} values derived from the most robust carcinogenicity datasets included in relevant carcinogenicity databases (EMA, 2024; Lhasa, 2023). NDELA has been detected in a variety of industrial and consumer products, including cutting fluids, cosmetics, tobacco, and some foods (IARC, 2000). Similarly, NPIP has been detected in a number of animal-based foods, drinking water, and tobacco smoke (EFSA, 2023; IARC, 1978). Both NDELA and NPIP were mutagenic in the presence and absence of metabolic activation in a variety of *in vitro* assays, positive in multiple *in vivo* assays, and are considered probably (NDELA; cat 2A) and possibly (NPIP, cat 2B) carcinogenic to humans by the International Agency for Research on Cancer Research (IARC) based on consistent and reproducible tumor production primarily in the liver, nasal cavity, and/or esophagus of rodents and hamsters in multiple carcinogenicity studies (as reviewed in EFSA, 2023; IARC, 1978 and 2000). Mutant frequency (MF) data obtained from the liver and stomach of Muta™Mouse transgenic mice after repeated dosing with NDELA and NPIP were analyzed using BMD modeling, and their respective BMD CIs were compared to those for NDMA and NDEA. The relative potencies of the mutagenicity and carcinogenicity values were evaluated for all four nitrosamines and compared with the outcomes of the CADRE model. The potential application of the relative potency comparison concept and derivation of health-protective AIs for mutagenic nitrosamines lacking specific *in vivo* carcinogenicity bioassay data is discussed.

2. MATERIALS AND METHODS

2.1. Transgenic Rodent Gene Mutation Assays

2.1.1. Test System (Muta™Mouse)

NDELA and NPIP were tested separately for mutagenicity in independent transgenic rodent bioassays. For each assay, the test system included 36 male CD_2-LacZ80/HazBR (Muta™Mouse) transgenic mice (Kobe Research Institute, Kobe-shi, Hyogo, Japan). All animals were identified with a unique identification number using a metal tag attached to the pinna of the ear. Animals with good health status were stratified into their respective study groups by body weight using a computer-generated randomization program (Provantis ™ Version 10.2.3.0). At the start of dosing, individual body weights ranged from 25.4 to 28.9 g for the NDELA groups, and from 25.3 to 29.7 g for the NPIP groups. Animals were socially housed in groups of 2 or 3 in polycarbonate caging with bedding material in a controlled environment at 20-26ºC (approximately 68-78ºF) and relative humidity of 30-70%, and with a 12-hour light/dark cycle. Animals were fed ad libitum with radiation-sterilized pelleted CRF-1 diet (Oriental Yeast Co., Ltd) and had free access to tap water.

2.1.2. Test Substance Characterization and Formulations

The chemical structures of NDELA (CAS No. 1116-54-7) and NPIP (CAS No. 100-75-4) are presented in Figure 1. NDELA was purchased from Veeprho Laboratories (Batch No. L34192) and NPIP was purchased from SynZeal Research Pvt. Ltd (Batch No. SRL-1112-137). NDELA is soluble in water at concentrations up to 100 mg/mL (NCBI, 2024a), and NPIP is soluble in aqueous media at concentrations up to 76.5 mg/mL (NCBI, 2024b). Therefore, NDELA formulations were prepared at concentrations ranging from 0.00250 mg/mL to 12.5 mg/mL in sterile water and NPIP formulations were prepared in 10% aqueous Tween 80 (Sigma Aldrich) at concentrations ranging from 0.002 mg/mL to 4 mg/mL. Based on historical information indicating aqueous formulations of both substances are stable at room temperature for at least 2 weeks in neutral or alkaline solutions when protected from light (IARC, 1978 and 2000), bulk NDELA and NPIP formulations were divided into aliquots for daily administration, stored at room temperature and protected from light, and used within 14 days of preparation. The positive control substance, N-ethyl-N-nitrosourea (ENU), was purchased from Toronto Research Chemicals Inc (Lot No. 2-GOP-61-7). ENU was formulated daily on each day of dosing at a concentration of 10 mg/mL in buffered sodium phosphate solution (pH 6).

2.1.3. Experimental Design

The in-life and lacZ gene mutant frequency (MF) analyses for both assays (NDELA and NPIP) were conducted at BioSafety Research Center

(Shizuoka, Japan) as summarized in Table I. The study design was compliant with the OECD Guideline for the Testing of Chemicals 488 (OECD, 2022). All animal procedures were conducted in accordance with regional animal welfare guidelines and standards for the care and management of laboratory animals (MOE, 2013 and 2014), and the study protocols were reviewed and approved by the test facility institutional animal care and use committee (IACUC) prior to initiation. Animals were dosed orally, by gastric intubation, once daily for 28 consecutive days with NDELA doses of 0 (control, sterile water), 0.025, 0.25, 2.5, 25 and 125 mg/kg/day, or with NPIP doses of 0 (control, 10% aqueous Tween 80) 0.02, 0.2, 2.0, 20 and 40 mg/kg/day, however based on an absence of increased MF from control at the dose level of 2.5 mg/kg/day in a preliminary assay, tissues from animals dosed with NDELA at 0.025 and 0.25 mg/kg/day were not subsequently evaluated. The dose volume was 10 mL/kg and individual dose volumes were calculated from the most recently recorded body weight. To minimize animal use in both assays, positive control DNA samples were obtained from 5 male animals (Muta™Mouse) from a similar study conducted at the same test facility in close temporal proximity to the NDELA and NPIP assays. Positive control animals were dosed for 2 consecutive days by intraperitoneal injection with 100 mg/kg (10 mL/kg) ENU followed by a 10-day manifestation period prior to tissue collection and preservation.

Group sizes were selected for consistency with current regulatory guidance for transgenic rodent mutagenicity assays (OECD, 2022) and to ensure adequate power to determine a dose range that elicits a meaningful biological difference (50% increase from the negative control group) for BMD modeling. Doses were selected based on a review of the available acute, *in vivo* mutagenicity, and repeated dose toxicity data, in addition to chronic and carcinogenicity study data for NDELA and NPIP (EFSA, 2023; IARC, 1978 and 2000; Totsuka et al., 2019). Specifically, the dose levels were selected to avoid exceeding a maximum tolerated dose (MTD) for repeated administration to mice, to bracket the cancer TD_{50} and/or BMD values used to derive the AIs for each substance (EMA, 2024; Lhasa, 2023), to ensure that at least one dose level represented a no-observed-genotoxic-effect-level (NOGEL), and to provide a sufficient number of adequately-spaced doses with a positive MF response to enable precise BMD-modeling and the estimation of meaningful BMD CIs (Slob, 2014).

2.1.4. Tissue Collection

Surviving animals were euthanized three days after administration of the last dose by inhalation of CO_2, followed by exsanguination. Samples of the liver (left lateral lobe) and stomach (glandular) were flash frozen in liquid nitrogen and stored frozen (-80°C) until processing for lacZ gene MF analysis. Liver and stomach were selected as the primary tissues for evaluation because the liver is a primary site of xenobiotic metabolism and a known target organ for carcinogenicity of NDELA and NPIP (IARC, 1978

and 2000), and the stomach is a site of early contact and considered to be exposed to high concentrations of orally administered substances.

2.1.5. DNA Extraction, Processing, and Analysis

Samples of frozen tissue from 5 animals/group dosed with NDELA, NPIP, or their respective vehicle control formulations were homogenized in a Dounce type homogenizer, and the homogenized cell fragments were centrifuged for 10 min at 1750 G. The nuclear/cell suspension was treated with proteinase K, and the solution was extracted twice with phenol/chloroform (1:1), and once with chloroform/isoamyl alcohol (24:1), with phase separation by centrifugation at 1750 G for 10 min after each extraction. Extracted genomic DNA was precipitated with 70% ethanol and pelleted by centrifugation at 13230 G for 10 min. Pelleted DNA was air dried, resuspended in TE buffer overnight at room temperature, analyzed for concentration using a spectrophotometer (NanoDrop®, ND-1000, AGC Techno Glass), adjusted to approximately 200 to 600 µg/mL with additional TE buffer and stored in a refrigerator (2-8°C) until used for packaging.

Approximately 2-6 µg of isolated DNA was packaged using Transpack packaging reagents (Agilent Technologies, Santa Clara, CA), and packaged phage particles of lambda shuttle vector DNA were incubated with *Escherichia coli C(lacZ⁻, gal E⁻)* in LB containing magnesium sulfate (10 mmol/L). After infection, the *E. coli* suspensions were mixed either with top agar containing Phenyl β-D-galactopyranoside (+P-gal) for determination of the number of mutant plaques, or with top agar without P-gal (-P-gal) for determination of the total number of plaques, plated on LB plates and incubated at 37°C overnight. After incubation, plaques present on both plates were manually enumerated, and the mutant frequency for each animal and tissue was calculated by dividing the number of mutant plaques (+P-gal) by the number of total plaque-forming units (pfu; -P-gal). Each experiment was completed with one or two packaging reactions to obtain a total pfu ≥ $3x10^5$ for all samples.

2.1.6. Statistical Analysis and Acceptability Criteria

Mutant frequency data for the vehicle control and nitrosamine treated groups were evaluated for homogeneity of variance using Bartlett's two-sided test with a significance level of 0.01 (Snedecor and Cochran, 1989). Non-homogenous data ($p \leq 0.01$ by Bartlett's test) were further analyzed using Steel's two-sided multiple comparison rank-sum test with a significance level of 0.05 (Steel, 1959). Additionally, a one-sided Cochran-Armitage trend test was conducted at a significance level of 0.025 (Armitage, 1955; Cochran, 1954). The vehicle and positive control (ENU) MF data were analyzed for homogeneity of variance using a two-sided F test with a significance level of 0.05, and non-homogenous data were compared using the two-sided Aspin-Welch *t* test with a significance level of 0.05 (Algina, 2005). Criteria for a valid test included that the MF in the positive

control group was significantly higher than the vehicle control group ($p \leq 0.05$), and that the MF for the vehicle control group was within the 95% confidence intervals of the test facility historical control data. Criteria for a positive mutagenicity response for nitrosamine-treated groups included a tissue-specific significantly higher MF ($p \leq 0.05$) compared with the vehicle control, evidence of a dose-response, and/or mean MF values outside the upper 95% CI of the test facility historical control data (Tables II and III).

2.2. Benchmark Dose Modeling

Mutant frequency data were further analyzed using the default and recommended settings within PROAST v70.1 (RIVM, 2022). Liver MF data for NDELA and liver and stomach MF data for NPIP were analyzed separately. Tab delimited mutant frequency and dose data for individual animals (n = 5/group) were imported into the PROAST web application (https://proastweb.rivm.nl) as point-separated text files, and a dose-response BMD analysis was performed. The critical effect size (CES)/benchmark response (BMR), a value which represents the degree of change defining a response in a given endpoint, was set to 50% (0.5) in for consistency with recent analyses (Bercu et al., 2023a; Chepelev et al., 2023; Douglas et al., 2022; Marchetti et al., 2021; White et al., 2025; Zhang et al., 2024). Model averaging, which provides a weighted average of the four best-fitting models based on the relative fit of each model to the data, was used in accordance with regulatory recommendations (EFSA, 2022). The number of bootstrap runs, or generated data sets based on the average model, was set to 200, and the critical Akaike's Information Criteria (AIC) difference (AIC criterion) was set to two. The BMD analysis was initiated in PROAST, and the Lower ($BMDL_{50}$) and upper ($BMDU_{50}$) confidence limits (CI) of the model averaged BMD were calculated and reported.

2.3. Quantum Mechanical Evaluation

2.3.1. Computational Modeling

The tiered structure of the N-nitrosamine model used in this evaluation and reported previously (Kostal and Voutchkova-Kostal, 2023) mimics that of other CADRE models (Graham et al., 2022; Kostal and Voutchkova-Kostal, 2016; Melnikov et al., 2024; Voutchkova-Kostal et al., 2022), relying on electronic structures of xenobiotics to model molecular interactions in the key events of metabolic pathways. The model assesses ionization and tautomer states relevant to the compound and uses aqueous Monte Carlo (MC) simulations in conjunction with mixed quantum and classical mechanics calculations (QM/MM) to compute physicochemical properties and solute-solvent energetics (i.e., Coulomb and van der Waals interactions). These simulations are based on an explicit water box with periodic boundaries, where rotations and translations of solute-surrounding water molecules are sampled, and the solute is evaluated with a

semiempirical QM method, sampling all bond lengths, angles and torsions. The solvent box and simulation length are determined by the volume of the N-nitrosamine, here requiring a ca. 20x20x20-Å box (comprising ~ 750 water molecules), $2x10^6$ configurations of solvent equilibration, $4x10^6$ configurations of system equilibration, and $8x10^6$ configurations of full-system averaging. Computed properties, including solute-solvent energies are thus ensemble averages, reflecting the dynamics of the system to better mimic biological conditions.

To capture reactivity, the CADRE model relies on the well-accepted QM-FMOT (Frontier Molecular Orbital Theory) approach (Kostal, 2018; LoPachin et al., 2011; Morell et al., 2014; Schieferdecker and Vock, 2025; Torrent-Sucarrat et al., 2010; Wondrousch et al., 2010), using global and atom-based steric factors and reactivity indices derived from nitrosamines' electronic structure. Electronic structures are calculated using density functional theory (DFT) with the mPW1PW91/MIDIX+ method, which was selected based on performance in Lewis-acid/base and hydrogen-abstraction reactions, considered relevant to the nitrosamine metabolic pathway (Kostal and Voutchkova-Kostal, 2023). In addition to predictive modeling, an electronic-structure read-across (ESRA) was used, which allows for comparison of structures based on their reactivity indices (and other properties derived from QM calculations) vs. similarity in atom-connectivity in a traditional read-across (Kostal and Voutchkova-Kostal, 2023).

2.3.2. Statistical Modeling

CADRE employs the R language (R, 2009) and environment for statistical computing (version 4.1.2), which is used for data analysis, linear regressions and linear discriminant analyses (LDAs). Multivariate normality (*mvn*) of descriptors is determined using functions in the *mvn* library, and where necessary, variables are transformed to a logarithmic scale. The original descriptor selection for the model was carried out with a genetic algorithm, as implemented in the library *genalg*, using 100 iterations with a mutation probability of 0.05 and the Bayesian Information Criteria (BIC) to avoid overfitting. Internal performance was estimated using the leave-one-out (LOO) cross-validation method. Final model selection was based on performance of the top 5 models in external validation (Kostal and Voutchkova-Kostal, 2023). The dataset used for model training was obtained from the Lhasa Carcinogenicity Database (LCDB, carcdb.lhasalimited.org), which contains model-relevant information on carcinogenicity potential and/or potency (Lhasa, 2023). The LDA models used in this study were trained to i) classify *N*-nitrosamine contaminants into 3 potency categories: potent cohort of concern (COC, Cat 1, $TD_{50} \leq 0.15$ mg/kg), COC compounds (Cat 2, $0.15 < TD_{50} \leq 1.5$ mg/kg), and non-COCs (Cat 3, $TD_{50} > 1.5$ mg/kg), and ii) distinguish carcinogens from true non-carcinogens. The CADRE toolkit also contains a multivariate linear regression (MLR) model, which was developed to predict TD_{50} values for potent nitrosamines without β-

hydrogens (TD_{50} < 1.5 mg/kg). The overall accuracy of the CADRE tool was reported to be 77% in external testing for the LDA models and >80% for the MLR model. Furthermore, CADRE extrapolation to the NDSRI space was explored and found to be reliable (Kostal and Voutchkova-Kostal, 2023), owing to the physics-led layup of the model, i.e., its reliance on the underlying chemistry (vs. chemicals in the training set).

3. RESULTS

3.1. TGR Assays

3.1.1. In-Life Parameters:

Except for one male animal administered NPIP at 40 mg/kg/day that was removed from study due to a moribund condition after 21 days of dosing, all animals survived to their scheduled necropsy. Tissues from this early decedent animal were not used for the subsequent mutant frequency evaluation. There were no clinical signs, effects on body wight or body weight gain, and no gross observations at necropsy at any NDELA dose level or at NPIP dosages of 2.0 mg/kg/day or less. Animals dosed with NPIP at 20 mg/kg/day had slightly lower cumulative body weight gains over the dosing period. The 40 mg/kg/day NPIP dosage was associated with cumulative body weight losses (Figure S1b), clinical observations of thinness, piloerection, and irregular respiration during the last week of dosing, and gross observations of focal patches of white discoloration in the forestomach.

3.1.2. Mutant Frequency Evaluation

As shown in Tables II and III, the mutant frequency (MF) assays were considered valid based on statistically significant ($p \leq 0.05$) increases in MF in the liver and stomach of the ENU positive control group relative to the vehicle group and observed mean vehicle control values were within the boundaries of the 95% CI of the test facility historical control data. As anticipated, administration of NDELA and NPIP was associated with dose-responsive higher MFs. NDELA produced statistically significant ($p \leq 0.05$) MF responses in the liver at doses of 25 and 125 mg/kg/day, but not at 2.5 mg/kg/day. There was no evidence of increased MF in the stomach at any NDELA dose level (Table II). NPIP was associated with statistically significantly higher ($p \leq 0.05$) MF in the liver and stomach at doses of 20 and 40 mg/kg/day (Table III), and a statistically significant ($p \leq 0.025$) trend toward a dose response was observed in the NDELA and NPIP liver MF data, and the NPIP stomach MF data. Based on the initial statistical analysis, the no-observed-genotoxic-effect-level (NOGEL) was considered to be 2.5 mg/kg/day for NDELA and 2.0 mg/kg/day for NPIP.

3.2. BMD Modeling

Individual liver MF data from NDELA-treated mice (Table II) and liver and stomach MF data from NPIP-treated mice (Table III) were also used for BMD modeling (PROAST v70.1) as described. For each analysis, four model families (exponential, lognormal, inverse exponential, and Hill) were fitted to the data (Figures 2, 3 and 4) and model weightings enabling the model-average process were derived based on goodness of fit. Individual model parameters are presented in Table IV, and the weights applied to each model are presented in Table V. Representative bootstrap curves comprising the BMD Confidence Interval ($BMDL_{50}$ – $BMDU_{50}$) ranges are presented in Figure 5a-c for NDELA liver MF, NPIP liver MF, and NPIP stomach MF, respectively. The model averaged BMD CI ($BMDL_{50}$ – $BMDU_{50}$) ranges for repeated administration to cause a 50% increase in MF from vehicle control in the liver were 6.6 to 17.3 mg/kg/day for NDELA and 2.3 to 8.7 mg/kg/day for NPIP (Table VII). The BMD range for a comparable change in the stomach of mice administered NPIP was 9.0 to 27.8 mg/kg/day.

3.3. Quantum Mechanical Evaluation

In assessing the underlying effects of the electronic structure, and by extension, the QM-derived indices of reactivity, it is imperative to start from an externally validated predictive model (here the CADRE model). As there are multiple steps in the bioactivation pathway for nitrosamines, each with differential significance depending on the nitrosamine structure, analysis of individual QM descriptors must be carried out post-prediction. Otherwise, one can end up ‘cherry-picking’ electronic (or physicochemical) properties that best support a pre-determined or ‘wishful’ outcome. To that end, the CADRE predictions for the 4 nitrosamine compounds (NDELA, NPIP, NDEA, and NDMA) were examined. In all cases, CADRE predicted the correct potency category for these compounds based on TD_{50} values in the LCDB. It should be noted, however, that NDEA and NDELA were used in the CARDRE training set, while NDMA and NPIP are in the model’s test (i.e., validation) set. Thus, this analysis is not a confirmation of the model’s predictive power; rather, knowing the model aligns well with reported potencies in the LCDB, the underlying drivers of this behavior may be interrogated.

In reducing the model to individual drivers of the predicted outcomes, it was observed that multiple indices and computed properties underscored the trend in metabolic activity (and by extension carcinogenicity) across the four compounds (Table VI). This is expected as there are multiple steps in nitrosamine metabolism.(Cross and Ponting, 2021) These descriptors were statistically validated within the CADRE model, and were used in a similar exercise to differentiate acyclic alkyl nitrosamines (Kostal and Voutchkova-Kostal, 2023), demonstrating their broader utility in this chemical space.

The first descriptor is the susceptibility to undergo radical chemistry at the α-carbon position, $f^0(C_\alpha) = [\rho_{N+1}(C_\alpha) + \rho_{N-1}(C_\alpha)]/2$, which reflects the initial C−H hydroxylation step using the Fukui function, $f(r) = \left[\frac{\partial\rho(r)}{\partial N}\right]_{v(r)}$, which in turn measures the propensity of an atomic position in the molecule to accept or donate electron density (Kostal and Voutchkova-Kostal, 2023). The second descriptor is the electrophilic susceptibility at the α-C, $f^+(C_\alpha) = [\rho_{N+1}(C_\alpha) - \rho_N(C_\alpha)]$, which gauges downstream conjugation with DNA by considering re-distribution of electron density across the molecule as a result of a nucleophilic attack (Kostal and Voutchkova-Kostal, 2023). Maxima in either susceptibility index correspond to greater propensity for this process. The third descriptor is the solvent-accessible volume area (SAVA) at the α-C and/or β-C (reflecting steric hinderance at this position). Lastly, in addition to metabolic reactivity, in Table VI we considered bioavailability via computed solute-solvent energetics, which were obtained from QM/MM/MC simulations as ensemble averages and further used to calculate hydrogen bonding between the nitrosamine and surrounding water molecules (Kostal and Voutchkova-Kostal, 2023).

4. DISCUSSION

The nitrosamine chemical class is considered by the ICH M7 (R2) guidance as part of a 'cohort of concern', indicating that standard safety concern thresholds cannot be applied (ICH, 2023). The ICH M7 Q&A (ICH, 2022) goes on to indicate that positive data from *in vivo* mutagenicity studies alone cannot be used to derive AIs for carcinogenicity. Furthermore, for all 'cohort of concern' classed substances, the only AI derivation pathways afforded by ICH M7 include extrapolation from substance-specific rodent carcinogenicity studies or read across to molecules that have adequate rodent carcinogenicity data. Some regulatory agencies, like the European Medicines Agency (EMA), Health Canada (HC), and the United States Food and Drug Administration (FDA) default to the carcinogenic potency categorization approach (CPCA; Chakravarti et al., 2024; EMA, 2024; Kruhlak et al., 2024; FDA, 2023) to define an AI. Additionally, EMA and HC currently accept negative *in vivo* mutagenicity test results as a basis for consideration of an NDSRI as a non-mutagenic impurity (NMI) and thus controllable according to ICH Q3B standards (EMA, 2024).

The carcinogenic potency of a nitrosamine is expected to be correlated to the *in vivo* mutagenicity potential because the mechanism by which a nitrosamine causes cancer is well understood (Li and Hecht, 2022; Snodin et al., 2024). Nitrosamines can be metabolically activated via cytochrome P450-mediated α-hydroxylation, a metabolic cascade that eventually results in the formation of the mutagenic alkyl diazonium, a potent DNA alkylating agent that can cause cell transformation and tumor formation (Li and Hecht, 2022; Snodin et al., 2024). Thus, the correlation between

carcinogenic potency and the *in vivo* mutagenic potency can be established by plotting the BMD values of anchor nitrosamines that have robust carcinogenicity data and *in vivo* mutagenicity data against their respective AIs. Figure 6 shows a graphical representation of the $BMDL_{50}$ and $BMDU_{50}$ ranges for four nitrosamines (NDEA, NDMA, NPIP and NDELA) plotted against their respective AI values. The weaker potency nitrosamines NDELA and NPIP have much higher AIs compared with the more potent nitrosamines NDEA and NDMA, indicating a precise relationship between the AIs derived from carcinogenicity data and the BMD CIs calculated from the TGR data. This relationship could likely be used to estimate the carcinogenic potency of any NDSRI that tests positive in an *in vivo* mutagenicity assay by comparing the BMD values of the NDSRI to the four anchor nitrosamines (NDELA, NPIP, NDMA and NDEA) and leveraging the empirical relationship between carcinogenic potency (as assessed by the AIs derived from carcinogenicity TD_{50} values) and mutagenic potency (as assessed by *in vivo* mutagenicity assays) for these anchor nitrosamines. For example, as shown in Table VII if a hypothetical nitrosamine impurity (NDSRI-1) has a $BMDL_{50}$ value of 100 mg/kg/day and a $BMDU_{50}$ value of 400 mg/kg/day, calculation of the NDSRI-1 AI values using the ratio of NDSRI-1/anchor nitrosamine $BMDL_{50}$ values and the anchor nitrosamine AIs yields comparable calculated NDSRI-1 AI values (within an order of magnitude) ranging from 26,500 to 68,900 ng/day. The most conservative AI of 26,500 ng/day, estimated from comparison with NDEA, can be used as the AI for NDSRI-1. Concurrent with this work, a similar approach was used to determine that the sitagliptin NDSRI impurity 7-nitroso-3-(trifluoromethyl)-5,6,7,8-tetrahydro[1,2,4]triazolo-[4,3-a]pyrazine (NTTP) is significantly less potent than its AI, derived using the CPCA approach, would suggest (Powley et al., 2024). Furthermore, another TGR-based approach was reported for the NDSRIs N-nitroso-fluoxetine, N-nitroso-duloxetine, and N-nitroso-atomoxetine which demonstrated that AIs for these NDSRIs, derived from *in vivo* mutagenicity data are higher than their respective CPCA-derived AIs (Jolly et al., 2024), suggesting they may be less potent than the CPCA calculation predicts. Addition of these NDELA and NPIP TGR results to the overall database of anchor nitrosamine mutagenicity data further extends the potency range evaluated and should increase the accuracy of AI estimates for NDSRIs based on *in vivo* mutagenic potency.

The assessment of NDSRI potency, and by extension, determination of AI, can be further supported by using a mechanistic, QM-based *in silico* model that exploits the same correlation between carcinogenic potency and *in vivo* mutagenicity. The CADRE tool, which was trained and externally validated using existing nitrosamines, correctly distinguished the potent NDEA and NDMA from the less potent NDELA and NPIP. To better understand these predictions, we scrutinized the underlying reactivity indices and relevant physicochemical properties to rationalize the observed difference in

metabolic activity and, by extension, carcinogenic potency. From Table VI, both radical and electrophilic susceptibility at the α-Cs showed that NDEA and NDMA are more reactive (larger index values) than either NDELA or NPIP. In contrast, SAVA at the α-C was not found to be a differentiating feature, except to note that the highest values (i.e., the smallest steric hinderance) was identified for NDMA (35.7 $Å^3$). Interestingly, SAVA at the β-C was markedly higher for NDEA (34.6 $Å^3$) than for NDELA (24.6 $Å^3$) or NPIP (21.4 $Å^3$); we previously indicated that this could reflect broader accessibility of the α-C region in the nitrosamine, which is relevant to reactivity, particularly when the interacting moiety (i.e., the heme group) is large (Kostal and Voutchkova-Kostal, 2023).

Estimating bioavailability from molecular simulations further supported the trend in reactivity metrics, as shown in Table VI by the computed nitrosamine-water Coulomb and Lennard-Jones interactions, which were obtained from energy-pair distributions. Simplified for the reader via hydrogen bond (H-bond) donors/acceptors, as calculated from radial distribution functions (rdfs), these metrics indicate that NDELA and NPIP are more water soluble (thus presumed to be less bioavailable) than NDEA/NDMA, where NDELA is the clear 'winner' due to the presence of two hydroxyl groups. As a side note, NPIP has a more water exposed *N*-nitroso group than its open-chain analogs, owing to the *syn* arrangement in the cyclic structure.

Overall, it can be concluded that the difference in potency is due to both reactivity (sterics and electronics) and bioavailability metrics, assuming no significant impacts of other metabolic pathways (e.g., hydroxy oxidation to aldehydes in NDELA). This analysis shows that to propose a mechanistically sound explanation for the differences in carcinogenicity, which is important when using BMD in lieu of TD_{50} values, a physics-led *in silico* approach useful even for small and structurally simple nitrosamines. Equally important, an externally validated QM model should always be preferred to a read-across, even if it is carried out at the electronic-structure level, as there are multiple confounding factors that affect the metabolic activation of nitrosamines.

A potential impact of underestimating AI values for NDSRIs, based on simplistic computational or structural approaches that tend to overestimate potency (i.e. non-QM methods), could include disruption of drug supplies and lack of patient access to critical and lifesaving medicines due to the inability of pharmaceutical manufacturers to meet strict regulatory limits (Robinson, 2024; Bharate, 2021). The relative potency hypothesis is therefore currently being assessed to determine whether potency defined using data from *in vivo* MF analyses corresponds to potency defined using data from *in vivo* cancer bioassays and derived human acceptable intakes (AIs). Potency is well-defined through the comparison of BMD CI between compounds, and here it is demonstrated that mutant frequency-based CI

potency relates well to established AIs. To use these mutation-defined metrics for risk assessment purposes, it is pragmatic and conservative to use the worst-case scenario metric of the mutant frequency analysis, which is the lower bound of the BMD CI ($BMDL_{50}$). The $BMDL_{50}$ is the recommended metric used for calculation of human health-based guidance values (HBGV; Johnson et al., 2014; MacGregor et al., 2015a; MacGregor et al., 2015b) and is proposed for use in the relative potency calculation to derive a human AI. The mathematical relationship between the *in vivo* mutant frequency $BMDL_{50}$ and human AI is supported by the mechanism of the nitrosamines under consideration. These substances are mutagenic carcinogens which act through induction of DNA adducts that when left unrepaired, or exceed the background level of endogenous adducts, results in increased mutant frequency throughout the genome. Mutations in genes linked to the hallmarks of cancer (e.g. over-expressed oncogenes driving uncontrolled cell division) can be induced by these compounds. Therefore, there is both a mathematical and mechanistic justification for calculation of human cancer-protective AIs from mutation data. The integration of validated QM models such as CADRE with *in vivo* studies is important both *a priori*, i.e., to gauge viability of a potentially higher, BMD-derived AI, as well as to establish a defensible, mechanistic interpretation of the outcomes post hoc. Crucially, this line of thinking is consistent with the current collaborative efforts between industry and regulators, which have highlighted the merits of QM in supporting (or correcting) the CPCA predictions and in helping elucidate the underlying SARs from first principles.

In summary, transgenic rodent liver mutant frequency (MF) data for the small nitrosamines NDELA and NPIP, with accompanying *in silico* QM results, contribute meaningful comparative information that expands the potency range of exemplar nitrosamine compounds. Points of departure (PODs) derived from *in vivo* mutagenicity assessments from these and other anchor nitrosamines can be compared for utility in deriving point of departure (PoD) metrics for nitrosamine drug substance-related impurities (NDSRIs). *In vivo* mutagenicity data for these nitrosamines correlates well with observed carcinogenicity results with respect to both relative and absolute potency. Notably, cross-species liver MF among rats and mice is remarkably similar for NPIP, demonstrating the precision and robustness of TGR-based evaluation and subsequent BMD analyses. The inclusion of NDELA MF and BMD CI ranges expands the carcinogenic potency range of tested anchor nitrosamines, which now encompasses several orders of magnitude between the highly potent nitrosamines such as NDMA and NDMA and the less potent NPIP and NDELA. These data should increase confidence in and provide additional support for including *in vivo* mutagenicity data in nitrosamine human health risk assessments, which has been a significant research focus for regulatory agencies, drug manufacturers and the scientific community, including the Health and

Environmental Institute (HESI) Genetic Toxicology Technical Committee (GTTC) (Gollapudi et al., 2013; Johnson et al., 2014), and the International Workshop on Genetic Toxicology (IWGT) (MacGregor et al., 2015a; MacGregor et al., 2015b). The anchor approach described herein exemplifies a conservative method for deriving an AI for an NDSRI. Additionally, these data will support ongoing comparative meta-analyses of *in silico*, *in vitro*, and *in vivo* (mutagenicity and carcinogenicity) data, undertaken by multi-stakeholder groups like the HESI GTTC and IWGT to expand the availability of risk assessment tools for this class of drug-related impurities. As consensus builds around the refinement of methods for derivation of AIs for NDSRIs without robust carcinogenicity data, evaluation and integration of novel methods to assess and characterize mutagenicity of NDSRIs (e.g., ecNGS, *in silico* QM, etc.) remains critical to correlate *in vitro* and *in vivo* results to reduce animal testing. With the rapid expansion of the knowledge base in this arena, flexibility, practicality, as well as robust science-based approaches are vital focal points.

5. AUTHOR CONTRIBUTIONS

All authors contributed to the manuscript by providing contributions to the study design, data analysis and interpretation; drafting, editing and/or reviewing the manuscript text, tables, and figures; and all authors approve the final submission.

6. ACKNOWLEDGEMENTS

The authors would like to thank Prasad Deshpande (Teva) for sourcing the NDELA and NPIP test substances, and Maya Ueda, M.S. (Transgenic, Inc. formerly BioSafety Research Center, Inc.) for overseeing the conduct of the transgenic rodent mutation assays and providing input and review of the Materials and Methods and Results sections of the manuscript.

7. FUNDING SOURCES

Funding for all activities described in this manuscript was provided by Teva Pharmaceutical Industries Ltd.

8. CONFLICT OF INTEREST

Authors J. Roper, T. Griffin, V. Niddam-Hildesheim, R. Nudelman, and G. Ott are or were employees, and are shareholders, of Teva Pharmaceutical Industries, a maker of human medicinal products. Authors G. Johnson, J. Kostal, and A Voutchkova-Kostal are expert consultants who evaluate risk associated with pharmaceutical impurities and are paid by Teva Pharmaceutical Industries.

REFERENCES

Algina J. (2005). Aspin–Welch Test. Available at: https://api.semanticscholar.org/CorpusID:118146341. Accessed 06 Feb 2024.

Armitage P. (1955). Tests for linear trends in proportions and frequencies. Biometrics 11:375-386.

Bercu JP, Masuda-Herrera M, Trejo-Martin A, Sura P, Jolly R, Kenyon M. (2023b) Acceptable intakes (AIs) for 11 small molecule N-Nitrosamines (NAs). Regulatory Toxicology and Pharmacology 142:105415. https://doi.org/10.1016/j.yrtph.2023.105415.

Bercu JP, Zhang S, Sobol Z, Escobar PA, Van P, Schuler M. (2023a) Comparison of the Transgenic Rodent Mutation Assay, Error Corrected Next Generation Duplex Sequencing, and the Alkaline Comet Assay to Detect Dose-Related Mutations Following Exposure to N-Nitrosodiethylamine. Mutation Research/Genetic Toxicology and Environmental Mutagenesis:503685.

Bharate SS. (2021) Critical Analysis of Drug Product Recalls due to Nitrosamine Impurities. Journal of Medicinal Chemistry, 64(6), 2923-2936. DOI: 10.1021/acs.jmedchem.0c02120.

Center for Research on Complex Generics (CRCG). (2024). Updates on Approaches to Acceptable Intakes of Nitrosamine Drug Substance Related Impurities (NDSRIs) and Bioequivalence Assessment for Reformulated Drug Products. https://www.complexgenerics.org/education-training/updates-on-approaches-to-acceptable-intakes-of-nitrosamine-drug-substance-related-impurities-ndsris-and-bioequivalence-assessment-for-reformulated-drug-products/. 06 November 2024.

Chakravarti S, Saiakhov RD, Girireddy M. (2024) Confidence score calculation for the carcinogenic potency categorization approach (CPCA) predictions for N-nitrosamines. Computational Toxicology 29:100298. https://doi.org/10.1016/j.comtox.2023.100298.

Chakravarti S, Saiakhov RD, Girireddy M. (2024). Confidence score calculation for the carcinogenic potency categorization (CPCA) predication for N-nitrosamines. Computational Toxicology, 29, 100298. https://doi.org/10.1016/j.comtox.2023.100298.

Chepelev N, Long AS, Beal M, Barton-Maclaren T, Johnson G, Dearfield KL. (2023) Establishing a quantitative framework for regulatory interpretation of genetic toxicity dose-response data: Margin of exposure case study of 48 compounds with both in vivo mutagenicity and carcinogenicity dose-response data. Environ Mol Mutagen 64(1):4-15.

Cochran WG (1954). Some methods of strengthening the common Chi-Square test. Biometrics 10:417-451.

Cross KP and Ponting DJ. (2021). Developing Structure-Activity Relationships for N-Nitrosamine Activity. Computational Toxicology. 20:100186. DOI: 10.1016/j.comtox.2021.100186.

Douglas GR, Beevers C. Gollapudi B, Keig-Shevlin Z. Kirkland D. O'Brien JM et al. (2022). Impact of sampling time on the detection of mutations in rapidly proliferating tissues using transgenic rodent gene mutation models: A review. Environmental and Molecular Mutagenesis, 63(8-9), 376–388. https://doi.org/10.1002/em.22514.

Dutch National Institute for Public Health and the Environment (RIVM). (2022) PROAST software package for the statistical analysis of dose-response data v70.1. Available online at: https://www.rivm.nl/en/proast. Accessed 23 October 2024.

European Food Safety Authority (EFSA). (2022) Guidance on the use of the benchmark dose approach in risk assessment. EFSA Journal, 20(10):7584 [67 pp.] Available online at: https://efsa.onlinelibrary.wiley.com/doi/pdf/10.2903/sp.efsa.2022.EN-7585. Accessed 23 October 2024.

European Food Safety Authority (EFSA). (2023) Risk assessment of N-Nitrosamines in food. EFSA Journal, 21(3):7884 [278 pp.] Available online at: https://efsa.onlinelibrary.wiley.com/doi/epdf/10.2903/j.efsa.2023.7884. Accessed 23 October 2024.

European Medicines Agency (EMA). (2024) Questions and answers for marketing authorization holders/applicants on the CHMP Opinion for the Article 5(3) of Regulation (EC) No 726/2004 referral on nitrosamine impurities in human medicinal products. EMA/409815/2020 Rev. 20. Available at https://www.ema.europa.eu/en/documents/referral/nitrosamines-emea-h-a53-1490-questions-and-answers-marketing-authorisation-holders-applicants-chmp-opinion-article-53-regulation-ec-no-726-2004-referral-nitrosamine-impurities-human-medicinal-products_en.pdf. Accessed 23 October 2024.

Food and Drug Administration (FDA).(2023) US Department of Health and Human Services. Recommended Acceptable Intake Limits for Nitrosamine Drug Substance Related Impurities (NDSRIs) Guidance for Industry. Available at: https://www.fda.gov/media/170794/download. Accessed 23 October 2024.

Food and Drug Administration. (2024). FDA-CDER and HESI: Nitrosamine Ames Data Review and Method Development Workshop. https://www.fda.gov/drugs/fda-cder-and-hesi-nitrosamine-ames-data-review-and-method-development-workshop-10152024%23event-information. October 15-16 2024.

Gollapudi BB, Johnson GE, Hernandez LG, Pottenger LH, Dearfield KL, Jeffrey AM. (2013) Quantitative approaches for assessing dose-response relationships in genetic toxicology studies. Environ Mol Mutagen 54(1):8-18.

Graham JC, Trejo-Martin A, Chilton ML, Kostal J, Bercu J, Beutner GL. (2022) An Evaluation of the Occupational Health Hazards of Peptide Couplers. Chem. Res. Toxicol. 35:6, 1011-1022. https://doi.org/10.1021/acs.chemrestox.2c00031.

ICHM7 (R2) Questions and Answers (Q&As). Step 4 version. (2022) Available at: https://database.ich.org/sites/default/files/M7R2_QAs_Step4_2022_0407.pdf. Accessed 23 October 2024.

ICHM7 (R2). (2023) Assessment and Control of DNA Reactive (Mutagenic) Impurities in Pharmaceuticals to Limit Potential Carcinogenic Risk. Final version. Adopted on 3 April 2023. Available At: https://database.ich.org/sites/default/files/ICH_M7%28R2%29_Guideline_Step4_2023_0216_0.pdf. Accessed 23 October 2024.

International Agency for Research on Cancer (IARC). (1978) IARC Monographs on the Evaluation of Carcinogenic Risks to Humans. Volume 17: N-Nitrosopiperidine (pp 287-301). World Health Organization, Lyon, France. Available at https://publications.iarc.fr/Book-And-Report-Series/Iarc-Monographs-On-The-Identification-Of-Carcinogenic-Hazards-To-Humans/Some-Em-N-Em--Nitroso-Compounds-1978. Accessed 23 October 2024.

International Agency for Research on Cancer (IARC). (2000) IARC Monographs on the Evaluation of Carcinogenic Risks to Humans. Volume 77: N-Nitrosodiethanolamine (pp 408-443). World Health Organization, Lyon, France. Available at https://publications.iarc.fr/95. Accessed 23 October 2024.

Johnson GE, Dobo K, Gollapudi B, Harvey J, Kenny J, Kenyon M. (2021). Permitted daily exposure limits for noteworthy N-nitrosamines. Environmental and Molecular Mutagenesis 62:5, p293-305. https://doi.org/10.1002/em.22446.

Johnson GE, Soeteman-Hernandez LG, Gollapudi BB, Bodger OG, Dearfield KL, Heflich RH. (2014) Derivation of point of departure (PoD) estimates in genetic toxicology studies and their potential applications in risk assessment. Environ Mol Mutagen 55(8):609-623.

Jolly RA, Cornwell PD, Noteboom J, Sayyed, FB, Thapa B, Buckley LA. (2024) Estimation of Acceptable Daily Intake Values based on Modeling and In Vivo Mutagenicity of NDSRIs of Fluoxetine, Duloxetine and Atomoxetine, Regulatory Toxicology and Pharmacology, 152:105672. https://doi.org/10.1016/j.yrtph.2024.105672.

Kostal J, Voutchkova-Kostal A, Bercu JP, Graham JC, Hillegass, J, Masuda-Herrera M, Trejo-Martin A, Gould J. (2024). Quantum-Mechanics Calculations Elucidate Skin-Sensitizing Pharmaceutical Compounds. Chem Res Toxicol, 37, 1404-1414.

Kostal J. and Voutchkova-Kostal A. (2016) CADRE-SS, an in Silico Tool for Predicting Skin Sensitization Potential Based on Modeling of Molecular Interactions. Chem. Res. Toxicol. 29:1, 58-64. https://doi.org/10.1021/acs.chemrestox.5b00392.

Kostal J. and Voutchkova-Kostal A. (2023) Quantum-Mechanical Approach to Predicting the Carcinogenic Potency of N-Nitroso Impurities in Pharmaceuticals. Chem. Res. Toxicol. 36:2, 291-304. https://doi.org/10.1021/acs.chemrestox.2c00380.

Kostal, J. (2018) Quantum Mechanics Approaches in Computational Toxicology. In Computational Toxicology, Ekins (Ed.). https://doi.org/10.1002/9781119282594.ch2.

Kruhlak NL, Schmidt M, Froetschl R, Graber S, Haas B, Horne I. (2024). Determining recommended acceptable intake limits for N-nitrosamine impurities in pharmaceuticals: Development and application of the Carcinogenic Potency Categorization Approach (CPCA). Regulatory Toxicology and Pharmacology, 150:105640. https://doi.org/10.1016/j.yrtph.2024.105640.

LHASA. (2023) Lhasa Carcinogenicity Database. Lhasa Limited. Available at https://carcdb.lhasalimited.org/. Accessed 23 October 2024.

Li, Y. and Hecht, SS. (2022) Metabolic Activation and DNA Interactions of Carcinogenic N-Nitrosamines to Which Humans Are Commonly Exposed. Int. J. Mol. Sci. 23, 4559. https://doi.org/10.3390/ijms23094559.

LoPachin RM, Gavin T, DeCaprio A, Barber DS. (2011). Application of the Hard and Soft, Acids and Bases (HSAB) Theory to Toxicant-Target Interactions. Chem. Res. Toxicol. 25:2, p239-251. https://doi.org/10.1021/tx2003257.

Lynch AM, Howe J, Hildebrand D, Harvey JS, Burman M, Harte DSG. (2024) N-Nitrosodimethylamine investigations in Muta™Mouse define point-of-departure values and demonstrate less-than-additive somatic mutant frequency accumulations. Mutagenesis. 2024 Jan 6:geae001. doi: 10.1093/mutage/geae001. Epub ahead of print. PMID: 38183622.

MacGregor JT, Frötschl R, White PA, Crump KS, Eastmond DA, Fukushima S. (2015a) IWGT Report on Quantitative Approaches to Genotoxicity Risk Assessment II. Use of Point-of-Departure (PoD) metrics in defining acceptable exposure limits and assessing human risk. Mutation Research - Genetic Toxicology 783:66-78.

MacGregor JT, Frötschl R, White PA, Crump KS, Eastmond DA, Fukushima S. (2015b) IWGT Report on Quantitative Approaches to Genotoxicity Risk

Assessment I. Methods and metrics for defining exposure-response relationships and points of departure (PoDs). Mutation Research - Genetic Toxicology 783:55-65.

Marchetti F. Zhou G. LeBlanc D. et al. (2021). The 28 + 28 day design is an effective sampling time for analyzing mutant frequencies in rapidly proliferating tissues of MutaMouse animals. Arch Toxicol 95, 1103–1116. https://doi.org/10.1007/s00204-021-02977-6.

Melnikov F, Kostal J, Voutchkova-Kostal A, Zimmerman JB, Anasta PT. (2016) Assessment of predictive models for estimating the acute aquatic toxicity of organic chemicals. Green Chem., 18, 4432-4445. https://doi.org/10.1039/C6GC00720A.

Ministry of the Environment (MOE). (2013) Standards relating to the Care and Keeping and Reducing Pain of Laboratory Animals (Notice of the Ministry of the Environment No. 88 of 2006). Latest revision: Notice of the Ministry of the Environment No. 84, Japan. [7 pp.] Available online at: https://www.env.go.jp/nature/dobutsu/aigo/2_data/laws/nt_h25_84_en.pdf. Accessed 23 October 2024.

Ministry of the Environment (MOE). (2014) Act on Welfare and Management of Animals (Act No. 105 of October 1, 1973). Latest revision: Act No. 46, Japan. [30 pp.] Available online at: https://www.env.go.jp/nature/dobutsu/aigo/1_law/files/aigo_kanri_1973_105_en.pdf. Accessed 23 October 2024.

Morell C, Gazquez JL, Vela A, Guegan F, Chermette H. 2014. Revisiting electroaccepting and electrodonating powers: proposals for local electrophilicity and local nucleophilicity descriptors. Phys. Chem. Chem. Phys. 16, p26832-26842. https://doi.org/10.1039/C4CP03167A.

National Center for Biotechnology Information (NCBI). (2024a). PubChem Compound Summary for CID 14223, N-Nitrosodiethanolamine. Available at https://pubchem.ncbi.nlm.nih.gov/compound/N-Nitrosodiethanolamine. Accessed 23 October 2024.

National Center for Biotechnology Information (NCBI). (2024b). PubChem Annotation Record for, N-NITROSOPIPERIDINE, Source: Hazardous Substances Data Bank (HSDB).Available at https://pubchem.ncbi.nlm.nih.gov/source/hsdb/5115. Accessed 23 October 2024.

Organization for Economic Cooperation and Development (OECD). (2014). Guidance Document on the Validation of (Quantitative) Structure-Activity Relationship [(Q)SAR] Models, OECD Series on Testing and Assessment, No. 69, OECD Publishing, Paris, https://doi.org/10.1787/9789264085442-en.

Organization for Economic Cooperation and Development (OECD). (2022) Test No. 488: Transgenic Rodent Somatic and Germ Cell Gene Mutation Assay, OECD Guidelines for the Testing of Chemicals, Section 4, OECD

Publishing, Paris, https://doi.org/10.1787/9789264203907-en. Accessed 23 October 2024.

Ponting DJ, Czich A, Felter SP, Glowienke S, Harvey JS, Nudelman R. (2024). Control of N-nitrosamine impurities in drug products: Progressing the current CPCA framework and supporting the derivation of robust compound specific acceptable intakes. Regulatory Toxicology and Pharmacology, 156, 105762. https://doi.org/10.1016/j.yrtph.2024.105762.

Powley MW, Sobol Z, Johnson GE, Clark, RW, Dalby SM, Ykoruk BA. (2024). N-Nitrosamine Impurity Risk Assessment in Pharmaceuticals: Utilizing In Vivo Mutation Relative Potency Comparison to Establish an Acceptable Intake for NTTP, Regulatory Toxicology and Pharmacology, 152, 105681. https://doi.org/10.1016/j.yrtph.2024.105681.

R. (2009) A language and environment for statistical computing, R Foundation for Statistical Computing: Vienna, Austria.

Robinson J. (2023) The Great Nitrosamine Audit: how many more drugs will disappear from our shelves? The Pharmaceutical Journal. Available at: https://pharmaceutical-journal.com/article/feature/the-great-nitrosamine-audit-how-many-more-drugs-will-disappear-from-our-shelves. Accessed on 01 November 2024.

Schieferdecker S, Vock E. (2025). Quantum Chemical Evaluation and QSAR Modeling of N-Nitrosamine Carcinogenicity. Chem. Res. Toxicol. 38:2, p325-339. https://doi.org/10.1021/acs.chemrestox.4c00476.

Slob W. (2014). Benchmark dose and the three Rs. Part II. Consequences for study design and animal use, Critical Reviews in Toxicology, 44:7, 568-580, DOI: 10.3109/10408444.2014.925424.

Snedecor GW and Cochran WG. (1989). Statistical Methods, Eighth Edition, Iowa State University Press.

Snodin DJ, Trejo-Martin A, Ponting DJ, Smith GF, Czich A, Cross K. (2024). Mechanisms of Nitrosamine Mutagenicity and Their Relationship to Rodent Carcinogenic Potency. Chem. Res. Toxicol. Publication Date: February 5, 2024. https://doi.org/10.1021/acs.chemrestox.3c00327.

Steel, RGD. (1959). A Multiple Comparison Rank Sum Test: Treatments versus Control. Biometrics 15(4):560-572. DOI 10.2307/2527654.

Thomas R, Ponting DJ, Thresher A, Schlingemann J, Wills JW, Johnson GE. (2025). Critical comparison of BMD and TD50 methods for the calculation of acceptable intakes for N-nitroso compounds. Arch Toxicol 99, 983-993. https://doi.org/10.1007/s00204-024-03951-8.

Thresher A, Foster R, Ponting DJ, Stalford SA Tennant RE, Thomas R. (2020) Are all nitrosamines concerning? A review of mutagenicity and carcinogenicity data. Regulatory Toxicology and Pharmacology, 116:104749. https://doi.org/10.1016/j.yrtph.2020.104749.

Torrent-Sucarrat M, De Proft F, Ayers PW, Geerlings P. (2010). On the applicability of local softness and hardness. Phys. Chem. Chem. Phys. 12, p1072-1080. https://doi.org/10.1039/B919471A.

Torro-Labbe A. (1999). Characterization of Chemical Reactions from the Profiles of Energy, Chemical Potential, and Hardness. J. Phys. Chem. A, 22, 4398-4403. https://doi.org/10.1021/jp984187g.

Totsuka Y, Lin Y, He Y, Ishino K, Sato H, Kato M. (2019). DNA Adductome Analysis Identifies N-Nitrosopiperidine Involved in the Etiology of Esophageal Cancer in Cixian, China. Chemical Research in Toxicology 2019 32 (8), 1515-1527. DOI: 10.1021/acs.chemrestox.9b00017.

Voutchkova-Kostal A, Vaccaro S, Kostal J. (2022). Computer-Aided Discovery and Redesign for Respiratory Sensitization: A Tiered Mechanistic Model to Deliver Robust Performance Across a Diverse Chemical Space. Chem. Res. Toxicol. 36:2, 291-304. https://doi.org/10.1021/acs.chemrestox.2c00224.

White PA, Chen G, Chepelev N, Bell MA, Gallant LR, Johnson GE. (2025) Benchmark Response (BMR) Values for In Vivo Mutagenicity Endpoints. Environ. Mol. Mutagen. Submitted and accepted, citation pending.

Wills J, Johnson GE, Battaion H, Slob W, White P. (2017). Comparing BMD-derived genotoxic potency estimations across variants of the transgenic rodent gene mutation assay. Environ Mol Mutagen 58:632-643.

Wondrousch D, Bohme A, Thaens D, Ost N, Schuurmann G. (2010). Local Electrophilicity Predicts the Toxicity-Relevant Reactivity of Michael Acceptors. J. Phys. Chem. Lett. 1:10, p1605-1610. https://doi.org/10.1021/jz100247x.

Zhang S, Coffing SL, Gunther WC, Homiski ML, Spellman RA, Van P, Schuler M. (2024). Assessing the genotoxicity of N-nitrosodiethylamine with three in vivo endpoints in male Big Blue® transgenic and wild-type C57BL/6N mice. Environ Mol Mutagen. Jul;65(6-7):190-202. doi: 10.1002/em.22615. Epub 2024 Jul 16. PMID: 39012003.

TABLES

Table I Study Design for Transgenic Rodent Mutation Assays with NDELA and NPIP

Species and Strain:	**Mouse/CD_2-LacZ80/HazfBR (Muta™Mouse) [SPF]**
Sex:	Male
Total animals used:	36 per assay - 72 total animals
Animals per group:	6[a]
Dose levels (mg/kg/day):	NDELA[b]: 0, 0.025, 0.25, 2.5, 25, or 125 mg/kg/day NPIP: 0, 0.02, 0.2, 2.0, 20 or 40 mg/kg/day
Vehicle:	NDELA: Sterile Water NPIP: 10% aqueous Tween 80
Route of administration:	Oral by gavage
Dosing regimen:	Once daily for 28 consecutive days
Positive control:	N-ethyl-N-nitrosourea (ENU)[c]
Dose volume (mL/kg):	10
Tissues sampled:	Liver and glandular stomach
Assay validity criteria:	Mutant frequency in the positive control group is statistically significantly higher than the vehicle control group. Mutant frequency in the negative control group is within the 95% control limits of the test facility historical control data.

[a] 6 mice/group were dosed. Mutant frequency was evaluated for 5 mice/group.
[b] NDELA dose levels of 0.025 and 0.25 mg/kg/day were not included in the MF evaluation because in an initial evaluation, an increase in MF compared to negative control was not observed in liver or stomach DNA samples of animals dosed with 2.5 mg/kg/day of NDELA.
[c] To reduce animal use, positive control DNA was obtained from the liver and stomach of 5 male mice (Muta™Mouse) from a separate TGR assay conducted at the same test facility which overlapped with the NDELA and NPIP TGR assays. Mice were dosed intraperitoneally with 100 mg/kg (10 mL/kg) ENU for 2 consecutive days followed by a 10-day manifestation period prior to tissue collection.

Table II Mutant Frequency (MF) Following Repeated Oral Administration of Vehicle Control, NDELA, or ENU Positive Control

Dose	Animal No.	Liver MF (x 10^{-6})		Stomach MF (x 10^{-6})	
		Individual	Mean (SD)	Individual	Mean (SD)
Vehicle Control[a] (Sterile WFI)	1001	30.8	37.1 (6.7)[b]	42.9	37.6 (6.1)
	1002	47.2		43.3	
	1003	31.3		34.2	
	1004	37.1		29.0	
	1005	39.1		38.4	
NDELA 2.50 (mg/kg/day)	1301	40.6	35.8 (4.0)	49.2	35.6 (7.8)
	1302	32.2		30.1	
	1303	33.3		34.5	
	1304	33.1		32.5	
	1305	39.6		31.8	
NDELA 25.0 (mg/kg/day)	1401	77.6	96.5 (19.0)[c]	41.2	36.7 (8.2)
	1402	96.8		46.7	
	1403	80.4		26.5	
	1404	124.4		30.3	
	1405	103.5		38.7	
NDELA 125 (mg/kg/day)	1501	415.2	378.3 (28.7)[c]	27.0	34.7 (8.1)
	1502	363.8		44.9	
	1503	348.1		41.7	
	1504	401.8		29.2	
	1505	362.0		30.5	
ENU[d] 100 (mg/kg/day)	PC01	108.4	134.3 (70.0)[e]	552.0	518.6 (65.3)[e]
	PC02	87.7		472.4	
	PC03	97.8		434.9	
	PC04	257.6		599.5	
	PC05	120.0		534.0	

[a] Historical control data ranges (Mean ± S.D.) were 38.9 ± 11.2 (x10^{-6}) for the liver and 38.0 ± 10.5 (x10^{-6}) for the stomach.
[b] statistically significant ($p \leq 0.025$) trend with increasing dose (Cochran Armitage trend test)
[c] statistically significant ($p \leq 0.05$) from vehicle control group (Steel's test)
[d] Historical control data ranges (Mean ± S.D.) were 120.9 ± 28.7 (x10-6) for the liver and 412.2 ± 84.6 (x10-6) for the stomach.
[e] statistically significant ($p \leq 0.05$) from vehicle control group (Aspin-Welch test)

Table III Mutant Frequency (MF) Following Repeated Oral Administration of Vehicle Control, NPIP or ENU Positive Control

Dose	Animal No.	Liver MF (x 10^{-6})		Stomach MF (x 10^{-6})	
		Individual	Mean (SD)	Individual	Mean (SD)
Vehicle Control[a] (10% aqueous Tween 80)	2001	33.2	31.6 (7.1)[b]	36.7	26.1 (7.0)[b]
	2002	41.2		25.6	
	2003	30.8		21.0	
	2004	31.4		28.5	
	2005	21.2		18.8	
NPIP 0.02 (mg/kg/day)	2101	18.1	32.6 (8.6)	32.7	35.7 (5.5)
	2102	35.7		31.2	
	2103	35.2		40.7	
	2104	40.8		42.7	
	2105	33.4		31.4	
NPIP 0.2 (mg/kg/day)	2201	30.4	33.2 (3.9)	23.2	30.6 (11.2)
	2202	32.7		18.2	
	2203	36.4		28.0	
	2204	28.6		45.9	
	2205	37.9		37.8	
NPIP 2.0 (mg/kg/day)	2301	29.6	65.9 (26.2)	32.4	30.0 (5.3)
	2302	103.5		28.6	
	2303	62.3		35.6	
	2304	68.0		21.7	
	2305	65.9		31.7	
NPIP 20 (mg/kg/day)	2401	202.7	145.1 (36.4)[c]	38.1	45.4 (6.7)[c]
	2402	147.4		44.8	
	2403	129.5		56.4	
	2404	142.3		43.8	
	2405	103.5		43.9	

Table III (continued): Mutant Frequency (MF) Following Repeated Oral Administration of Vehicle Control, NPIP or ENU Positive Control (Continued)

Dose	Animal No.	Liver MF (x 10^{-6})		Stomach MF (x 10^{-6})	
		Individual	Mean (SD)	Individual	Mean (SD)
NPIP 40 (mg/kg/day)	2501	475.2	741.5 (176.8)[c]	72.9	76.9 (28.1)[c]
	2502	767.4		53.1	
	2503	757.8		58.6	
	2504	972.0		75.6	
	2505	734.9		124.3	
ENU[d] 100 (mg/kg/day)	PC01	125.5	174.8 (90.6)[e]	358.8	414.1 (52.6)[e]
	PC02	133.3		418.6	
	PC03	137.3		364.0	
	PC04	336.6		476.5	
	PC05	141.4		454.0	

[a] Historical control data ranges (Mean ± S.D.) were 38.9 ± 11.2 (x10-6) for the liver and 38.0 ± 10.5 (x10-6) for the stomach.
[b] statistically significant ($p \leq 0.025$) trend with increasing dose (Cochran Armitage trend test)
[c] statistically significant ($p \leq 0.05$) from vehicle control group (Steel's test)
[d] Historical control data ranges (Mean ± S.D.) were 120.9 ± 28.7 (x10-6) for the liver and 412.2 ± 84.6 (x10-6) for the stomach.
[e] statistically significant ($p \leq 0.05$) from vehicle control group (Aspin-Welch test)

Table IV Individual Model Output Parameters Applied in PROAST v70.1 for Benchmark Dose Analysis of NDELA and NPIP Mutant Frequency Data

	Model	loglik	AIC	var	a	b	c	d	CED	CEDL	CEDU
NDELA (Lv)	Inverse Exp.	11.99	-13.98	0.01765	35.61	63.72	124.4	0.5	10.39	7.34	12.7
	Lognormal	12.14	-14.28	0.01739	35.92	0.02889	13.63	1	12.55	7.82	14.3
	Exponential	12.20	-14.40	0.01729	36.11	28.36	10.45	5	20.34	8.78	21
	Hill	12.19	-14.38	0.01730	36.09	27.88	10.62	3.333	17.39	8.51	18.5
NPIP (Lv)	Inverse Exp.	-10.63	29.26	0.11890	36.91	627.7	$1x10^{18}$	0.3533	8.22	2.05	12.1
	Lognormal	-9.77	27.54	0.11230	35.55	0.04486	$1x10^{18}$	0.4427	5.69	1.69	10.3
	Exponential	-8.30	24.60	0.10180	34.26	726.6	$1x10^{18}$	0.897	4.20	1.53	8.05
	Hill	-8.43	24.86	0.10270	34.40	640	$1x10^{18}$	0.9252	4.35	1.58	8.26
NPIP (St)	Inverse Exp.	-0.81	9.62	0.06182	29.58	6086	$1x10^{18}$	0.2667	19.48	10.3	27.1
	Lognormal	-0.82	9.64	0.06185	29.53	0.02578	$1x10^{18}$	0.4457	19.48	10.2	27.4
	Exponential	-0.85	9.70	0.06195	29.44	1109	$1x10^{18}$	1.144	19.5	9.61	27.9
	Hill	-0.85	9.70	0.06194	29.44	1072	$1x10^{18}$	1.152	19.5	9.62	27.9

Abbreviations: Lv = liver; St = stomach; loglik = log-likelihood (goodness of fit); AIC = Akaike's Information Criterion; var = variance of model residuals; a = model intercept parameter; b = model slope parameter; c and d = dose-response curve shape parameters; CED = Critical Effect Dose (mg/kg/day); CEDL = Lower confidence limit of the CED (mg/kg/day); CEDU = Upper confidence limit of the CED (mg/kg/day).

Table V Model Weighting Applied in PROAST v70.1 for Benchmark Dose Model Averaging of NDELA and NPIP Mutant Frequency Data

	NDELA	NPIP	
Model	**Liver**	**Liver**	**Stomach**
Exponential	0.2672	0.4534	0.2456
Hill	0.2645	0.3982	0.2456
Inverse Exponential	0.2166	0.0441	0.2556
Lognormal	0.2516	0.1043	0.2531

Model weights are based on the relative goodness of fit of each model to the data.

Table VI Electronic, Steric and Physicochemical Properties of NDELA, NPIP, NDEA and NDMA

	Radical susceptibility (α-C)	**Electrophilic susceptibility (α-C)**	**SAVA, α-C/β-C (Å^3)**	**E_{Coul} / E_{LJ} (kcal/mol)**	**$E_{solute-solvent}$ (kcal/mol)**	**H-bond donor**	**H-bond acceptor**
NDMA	0.046	0.049	35.7/ -	-18.9/-7.3	-26.2	0	3.1
NDEA	0.032	0.041	20.4/34.6	-21.1/-10.2	-31.3	0	3.3
NPIP	0.030	0.028	22.4/21.4	-22.6/-10.8	-33.4	0	3.8
NDELA	0.026	0.025	20.5/24.6	-47.4/-7.9	-55.3	1.9	6.7

Electronic, steric and physicochemical properties computed for NDELA, NPIP, NDEA and NDMA to aid in electronic-structure read-across (ESRA) to explain the difference in potencies between NDELA/NPIP and NDEA/NDMA. Maximal radical susceptibility at the α-C = $f^0(C_\alpha)$ = $[\rho_{N+1}(C_\alpha) + \rho_{N-1}(C_\alpha)]/2$; Maximal electrophilic susceptibility at the α-C = $f^+(C_\alpha)$ = $[\rho_{N+1}(C_\alpha) - \rho_N(C_\alpha)]$; SAVA = solvent-accessible volume area; E_{Coul} = Coulomb energetics between the nitrosamine and surrounding water molecules; E_{LJ} = Lennard-Jones energetics between the nitrosamine and surrounding water molecules; $E_{solute-solvent}$ = sum of Coulomb and LJ energies; H-bond = number of hydrogen bond interactions computed from radial distributions functions (rdfs).

Table VII Acceptable Intake Estimates for a Putative NDSRI (NDSRI-1) Using BMD Modeling and Acceptable Intakes for the Anchor Nitrosamines NDELA, NPIP, NDMA, and NDEA

Anchor Nitrosamine	AI[a] (ng/day)	Transgenic Rodent Assay BMD CIs (mg/kg/day)[b]		$BMDL_{50}$ Ratio (NDSRI-1/Anchor)	NDSRI-1 AI (ng/day)
		$BMDL_{50}$	$BMDU_{50}$		
NDELA	1900	6.6	17.3	15	28500
NPIP	1300	2.3	8.74	43	55900
NPIP[c]	1300	1.89	3.61	53	68900
NDMA[d]	96[e]	0.21	0.46	476	45696
NDEA[f]	26.5[e]	0.1	1	1000	26500
NDSRI-1	-	100	400	-	-

[a] All acceptable intake values are from EMA, 2024.
[b] BMD Confidence Intervals (CI) are based on mutant frequencies from liver tissue
[c] BMD CI values are from Powley et al., 2024.
[d] BMD CI values are from Lynch et al., 2024.
[e] Although the acceptable intake values recognized by relevant Health Authorities are represented in the table, alternate AI values of 145 ng/day for NDMA and 62 ng/day for NDEA have been proposed based on subsequent review of available carcinogenicity studies in the LHASA database (Bercu et al., 2023b).
[f] BMD CI values are from Bercu et al., 2023a.

FIGURE LEGENDS

Figure 1: Chemical structures of: a) N-nitrosodiethanolamine (NDELA; CAS No. 1116-54-7) and b) N-nitrosopiperidine (NPIP; CAS No. 100-75-4).

Figure 2: Individual model output from BMD analysis of NDELA mutant frequency data using PROAST v70.1 (https://proastweb.rivm.nl). The four best-fitting models were: a) inverse exponential, b) lognormal, c) exponential, and d) Hill. Small triangles represent individual liver MF values, large triangles represent group mean MF values, horizontal dashed lines represent the critical effect size (50% increase from vehicle control), and vertical dashed lines represent the dose at which the critical effect is achieved. Individual model output parameters are described in Table IV, and results were used for model averaging (Figure 5a) and estimation of the $BMDL_{50}$ and $BMDU_{50}$ values (Table VII).

Figure 3: Individual model output from BMD analysis of NPIP mutant frequency data using PROAST v70.1 (https://proastweb.rivm.nl). The four best-fitting models were: a) inverse exponential, b) lognormal, c) exponential, and d) Hill. Small triangles represent individual liver MF values, large triangles represent group mean MF values, horizontal dashed lines represent the critical effect size (50% increase from vehicle control), and vertical dashed lines represent the dose at which the critical effect is achieved. Individual model output parameters are described in Table IV, and results were used for model averaging (Figure 5b) and estimation of the $BMDL_{50}$ and $BMDU_{50}$ values (Table VII).

Figure 4: Individual model output from BMD analysis of NPIP mutant frequency using PROAST v70.1 (https://proastweb.rivm.nl). The four best-fitting models were: a) inverse exponential, b) lognormal, c) exponential, and d) Hill. Small triangles represent individual liver MF values, large triangles represent group mean MF values, horizontal dashed lines represent the critical effect size (50% increase from vehicle control), and vertical dashed lines represent the dose at which the critical effect is achieved. Individual model output parameters are described in Table IV, and results were used for model averaging (Figure 5c) and estimation of the $BMDL_{50}$ and $BMDU_{50}$ values (Table VII).

Figure 5: Benchmark Dose (BMD) model averaging output for: a) liver mutant frequency (MF) data from transgenic mice administered NDELA, and b) liver and c) stomach MF data from mice administered NPIP. Individual MF data were resampled with replacement against the weighted averages (Table V) of the four best fitting models (Figures 2, 3, and 4) to generate 200 individual bootstrap curves which were used to estimate the BMD confidence intervals ($BMDL_{50}$ and $BMDU_{50}$), represented by the horizontal black bar beneath each set of curves.

Figure 6: Comparison of the mutant frequency (MF) benchmark dose (BMD) confidence interval (CI) ranges and acceptable intake (AI) values for

four anchor nitrosamines. Black lines represent Log_{10} transformed liver MF BMD CI intervals ($BMDL_{50}$ – $BMDU_{50}$) as described in Table VII. [a] Data from Bercu et al., 2023a. [b] Data from Lynch et al., 2024. [c] Data from Powley et al., 2024.

SUPPLEMENTAL FIGURE LEGEND

Figure S1: Group mean body weights (Day 1 to 31; g) of transgenic mice administered a) NDELA or b) NPIP for 28 consecutive days followed by a 3-day manifestation period prior to tissue collection for mutant frequency evaluation.

FIGURES

Figure 1: Chemical Structures of NDELA and NPIP

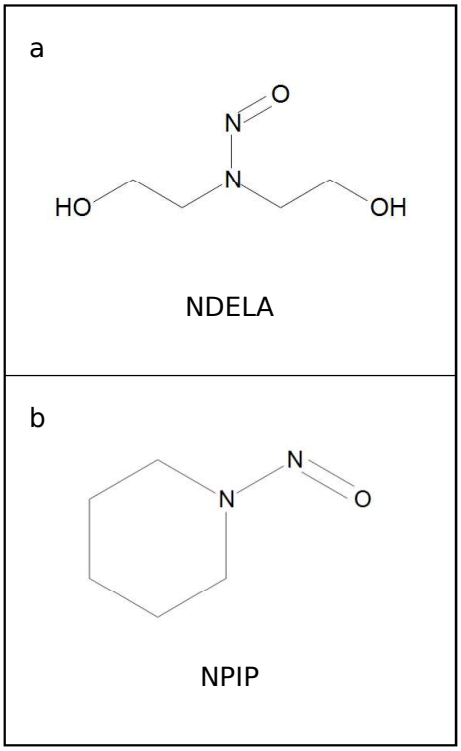

Figure 2: Benchmark Dose Analysis (PROAST v70.1) of Mutant Frequency Data from Liver of Transgenic Mice After Repeated Oral Administration of NDELA

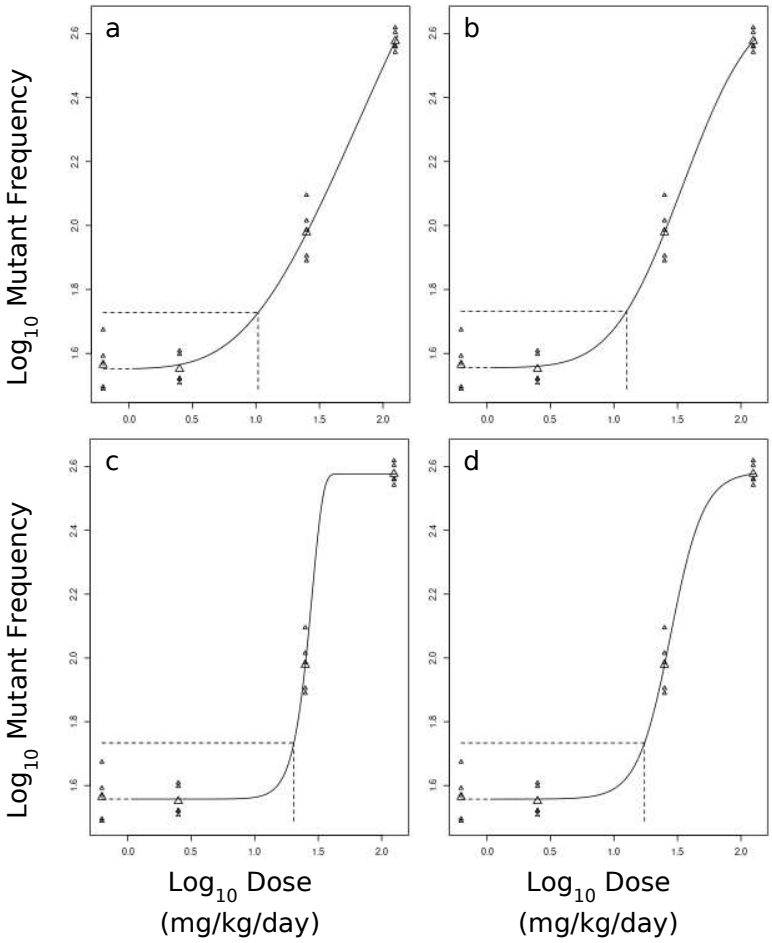

Figure 3: Benchmark Dose Analysis (PROAST v70.1) of Mutant Frequency Data from Liver of Transgenic Mice After Repeated Oral Administration of NPIP

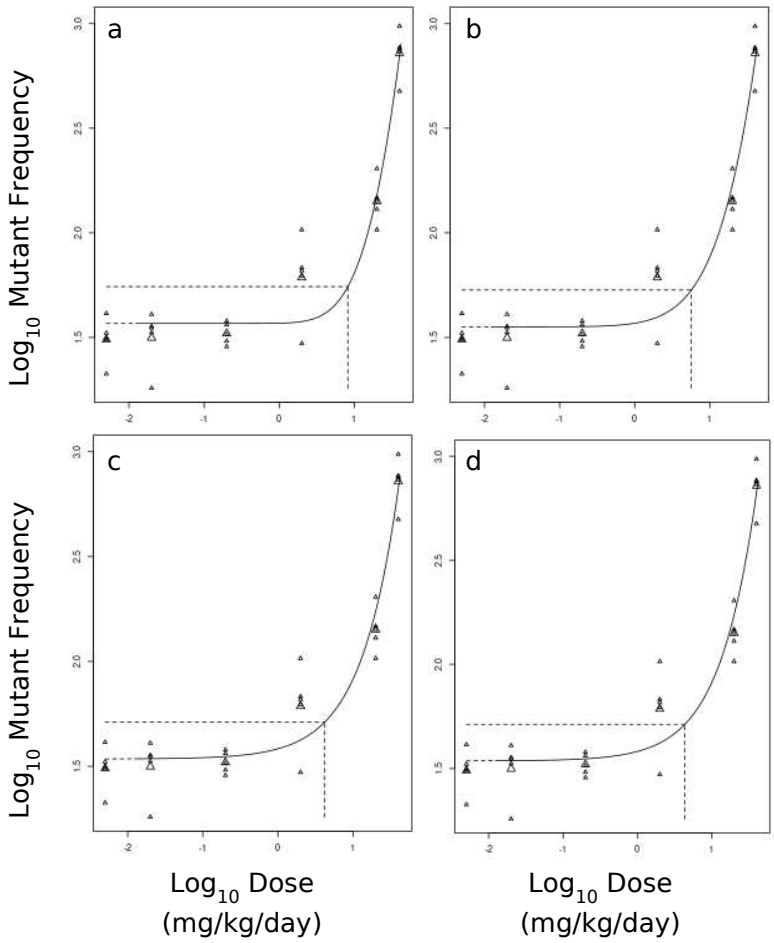

Figure 4: Benchmark Dose Analysis (PROAST v70.1) of Mutant Frequency Data from Stomach of Transgenic Mice After Repeated Oral Administration of NPIP

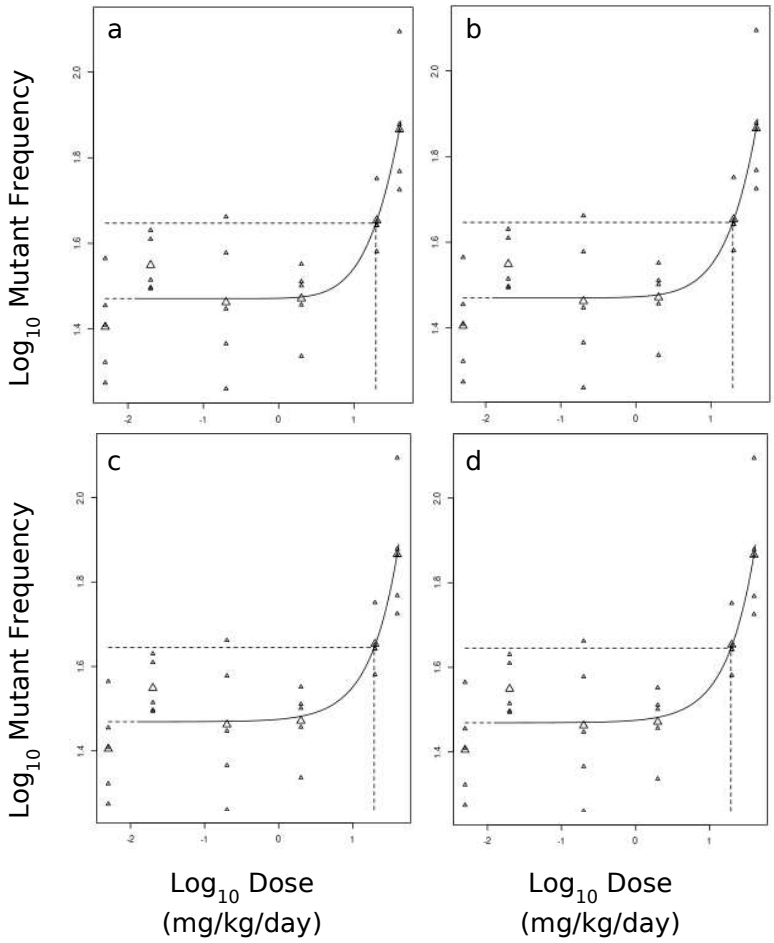

Figure 5: Benchmark Dose Model Averaging Analysis of Liver and Stomach Mutant Frequency Data from Transgenic Mice After Repeated Oral Administration of NDELA and NPIP

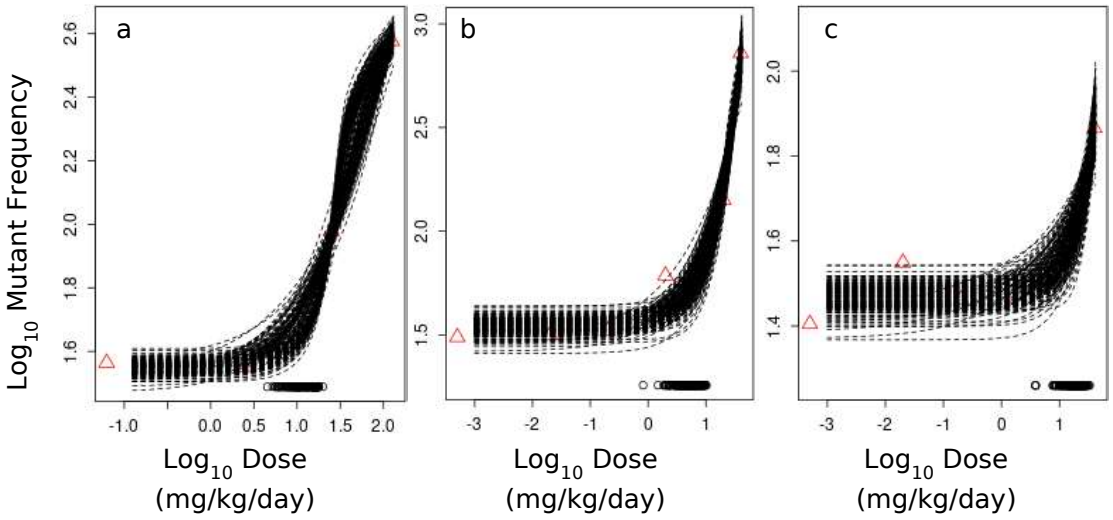

Figure 6: Correlation Between Liver $BMDL_{50}$ and $BMDU_{50}$ Values of Anchor N-Nitrosamines and Their Respective Acceptable Intakes